

# $UBV(RI)_C$ photometric comparison sequences for symbiotic stars<sup>★</sup>

A. Henden<sup>1</sup> and U. Munari<sup>2</sup>

<sup>1</sup> Universities Space Research Association/U.S. Naval Observatory Flagstaff Station, P.O. Box 1149, Flagstaff AZ 86002-1149, U.S.A.

<sup>2</sup> Osservatorio Astronomico di Padova, Sede di Asiago, I-36012 Asiago (VI), Italy

Received January 14; accepted January 31, 2000

**Abstract.** We present accurate  $UBV(RI)_C$  photometric sequences around 20 symbiotic stars. The sequences extend over wide brightness and color ranges, and are suited to cover quiescence as well as outburst phases. The sequences are intended to assist both present time photometry as well as measurement of photographic plates from historical archives.

**Key words:** catalogs — stars: binaries: symbiotic — techniques: photometric

## 1. Introduction

Symbiotic stars are binary systems composed of a cool giant and a hot, luminous white dwarf. They show variability over any time scale from minutes (flickering) to several decades (outbursts of symbiotic novae), with phenomena related to the orbital motion having periodicities generally between 1 and 4 years (or a few decades in the systems harbouring a Mira variable,  $\sim 20\%$  of all known symbiotic stars).

Such long time scales tend to discourage stand-alone photometric campaigns from a single Observatory (which would require observational programs running up to  $\sim 10$  years in order to derive - for example - a firm orbital period). Most of the current photometric investigations of symbiotic stars therefore try to assemble as much as possible data from the widest set of current and archival sources. A template example is the recent reconstruction of the 1890-1996 lightcurve and orbital period determination for YY Her by Munari et al. (1997).

*Send offprint requests to:* U. Munari

<sup>★</sup> Tables also available at CDS via anonymous ftp to cdsarc.u-strasbg.fr (130.79.128.5) or via <http://cdsweb.u-strasbg.fr/Abstract.html>

The data so collected are generally very heterogeneous in nature, with large differences caused for example by (a) the non-standard photometric bands, (b) the adopted comparison sequences and standard stars, (c) lack of adherence to and transformation into a system of general use, like the  $UBV(RI)_C$ , and (d) telescope focal length or pixel scale that causes blending with images of nearby field stars. These differences generally may introduce such a large scatter in the data that all but the strongest details are washed out.

The establishment of suitable and accurate photometric comparison sequences covering a wide range in magnitude and colors should alleviate considerably some of the above problems, and could encourage small observatories and/or occasional observers to obtain new data as well as to encourage those with access to plate archives to search for valuable historical data.

To this aim we present here suitable,  $UBV(RI)_C$  comparison sequences for 20 symbiotic stars (all but a few accessible from both hemispheres. See Table 1 for a list of the program stars). The sequences are basically intended to allow a general observer to capture on a single CCD frame or to have in the same eyepiece field of view when inspecting archival photographic plates: (a) enough stars to cover the whole range of known or expected variability for the given symbiotic star, (b) stars of enough different colors to be able to calibrate the instrumental color equations and therefore reduce to the standard  $UBV(RI)_C$  system the collected data, and (c) stars well separated from surrounding ones to avoid blending at all but the shortest telescope focal lengths.

## 2. Observations

All observations were made with the 1.0-m Ritchey-Chrétien telescope of the U.S. Naval Observatory, Flagstaff Station. A Tektronix/SITe 1024  $\times$  1024 thinned,

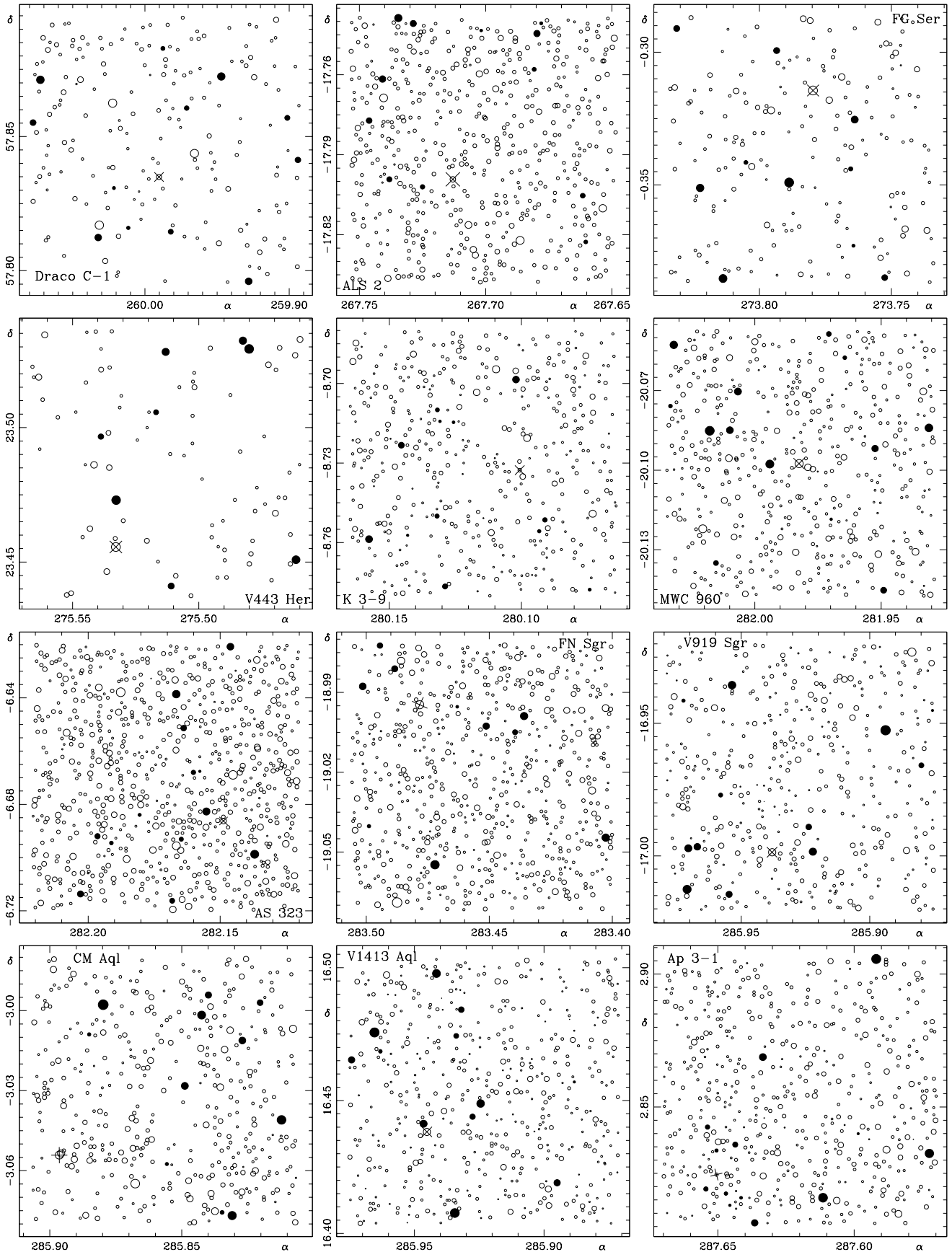


**Fig. 1.** Finding charts for the  $UBV(RI)_C$  comparison photometric sequence around the program symbiotic stars. The fields are in the same order as in Table 1. North is up and East to the left, with an imaged field of view of  $5.16 \times 5.16$  arcmin and a  $5.4 \times 5.4$  coordinate grid (see bottom-right panel of Fig. 2). Stars are plotted as open circles of diameter proportional to the brightness in the  $V$  band. The stars making up the photometric sequence (see Table 2) are plotted as filled circles

**Table 1.** List of program symbiotic stars. The coordinates for the symbiotic stars are from our observations (equinox J2000.0, mean epoch 1999.5). The  $e_\alpha$  and  $e_\delta$  columns list the errors in milliarcsec for right ascension and declination, respectively. The last two columns list the coordinates of the field centers in Figs. 1 and 2

names	star coordinates								field center		
	$\alpha$ (J2000.0)	$\delta$	$\alpha$ (J2000.0)	$\delta$	$e_\alpha$	$e_\delta$	$l$	$b$	$\alpha$ (J2000.0)	$\delta$	
Draco C-1	Stetson 3203	259.990265	+57.834927	17 19 57.661	+57 50 05.74	8	15	86.27	+34.76	259.9870	+57.8445
ALS 2	SS 324	267.712982	-17.799196	17 50 51.123	-17 47 57.11	26	61	10.18	+4.70	267.7010	-17.7881
FG Ser	AS 296	273.779633	-0.314434	18 15 07.121	-00 18 51.96	41	12	28.48	+7.93	273.7840	-0.3367
V443 Her	MWC 603	275.532837	+23.455601	18 22 07.883	+23 27 20.16	25	11	1.23	+16.59	275.5130	+23.4869
K 3-9	Sa 3-142	280.100555	-8.732704	18 40 24.133	-08 43 57.73	214	166	23.91	-1.54	280.1145	-8.7303
MWC 960	SS 174	281.982544	-20.097490	18 47 55.802	-20 05 50.97	38	28	14.53	-8.27	281.9820	-20.0976
AS 323	MH $\alpha$ 369-39	282.148712	-6.686234	18 48 35.689	-06 41 10.44	220	144	26.66	-2.41	282.1705	-6.6700
FN Sgr	AS 329	283.478241	-18.994621	18 53 54.780	-18 59 40.64	70	157	16.15	-9.06	283.4530	-19.0219
V919 Sgr	AS 337	285.937988	-16.998638	19 03 45.110	-16 59 55.10	48	4	19.01	-10.32	285.9270	-16.9705
CM Aql		285.896393	-3.054159	19 03 35.133	-03 03 14.97	150	129	31.59	-4.09	285.8565	-3.0300
V1413 Aql	AS 338	285.945160	+16.438210	19 03 46.840	+16 26 17.55	22	14	48.97	+4.77	285.9230	+16.4538
Ap 3-1		287.650543	+2.824543	19 10 36.122	+02 49 28.36	65	86	37.64	-2.97	287.6200	+2.8560
ALS 1	PK 028-09.3	289.067047	-8.296070	19 16 16.087	-08 17 45.85	0	15	28.30	-9.27	289.0820	-8.2958
V335 Vul	AS 356	290.808868	+24.461161	19 23 14.124	+24 27 40.17	46	39	58.22	+4.40	290.8060	+24.5000
QW Sge	AS 360	296.456451	+18.613464	19 45 49.548	+18 36 48.47	60	146	55.64	-3.02	296.4660	+18.6330
LT Del	He2-467	308.988495	+20.191086	20 35 57.234	+20 11 27.91	30	15	63.40	-12.15	309.0170	+20.1800
Hen 2-468		310.329163	+34.747917	20 41 18.989	+34 44 52.52	32	27	75.94	-4.44	310.3230	+34.7710
V407 Cyg	AS 453	315.540955	+45.775787	21 02 09.831	+45 46 32.85	11	15	86.99	-0.49	315.5030	+45.7730
V627 Cas	AS 501	344.420868	+58.820168	22 57 41.002	+58 49 12.60	45	86	108.66	-0.86	344.3940	+58.8465
StH $\alpha$ 32		69.440117	-1.319949	04 37 45.628	-01 19 11.82	57	11	197.48	-30.04	69.4312	-1.3413

backside-illuminated CCD was used, along with Johnson  $UBV$  and Kron-Cousins  $RI$  filters. Images were processed using IRAF, with nightly median sky flats and bias frames. Aperture photometry was performed with routines similar to those in DAOPHOT (Stetson 1987). Astrometry was performed using SLALIB (Wallace 1994) linear plate transformation routines in conjunction with the USNO-A2.0 reference catalog. Errors in coordinates were typically under 0.1 arcsec in both coordinates, referred to the mean coordinate zero point of the reference stars in each field.

The telescope scale is 0.6763 arcsec/pixel, with a total field of view of around  $11.4 \times 11.4$  arcmin. Typical seeing was  $\sim 2$  arcsec. A 9 arcsec extraction aperture with concentric sky annulus was commonly used.

The reported photometry only uses data collected on photometric nights (transformation errors under 0.02 mag). For each such night, symbiotic field observations were interspersed with observations of Landolt (1983, 1992) standard fields, selected for wide color and airmass range. The mean transformation coefficients (cf. Henden & Kaitchuck 1990, Eqs. 2.9ff) are:

$$\begin{aligned}
 V &: -0.020 \pm 0.007 & (1) \\
 B - V &: 0.949 \pm 0.007 & (2) \\
 U - B &: 1.072 \pm 0.018 & (3) \\
 V - R &: 1.017 \pm 0.005 & (4) \\
 R - I &: 0.971 \pm 0.013. & (5)
 \end{aligned}$$

Second order extinction was negligible except for  $B-V$ , where a coefficient of  $-0.03$  was used.

The symbiotic field photometry was usually performed as the field transited. In a few rare cases, observations were made at higher airmass to the West. In these cases, care was taken to obtain extinction measures at equivalent or higher airmass. Each field was observed on at least three nights. Since all primary standards used the same aperture as the secondary standards being established, and the apertures were large, no aperture corrections were necessary.

### 3. The photometric sequences

Between 10 and 15 stars around each symbiotic star have been selected to form the comparison sequences, given in Table 2. The sequences have been selected and ordered on the basis of the  $B$  magnitude. The  $B$  magnitude is reproducible by most filter-equipped CCD cameras, it is the closest one to the  $m_{pg}$  band of the historical photographic observations and the  $B$  band is particularly well suited to investigate the variability of symbiotic stars (see next section).

The range in magnitude of the sequences is large enough to cover both outburst and quiescence phases (eclipses included) of each symbiotic star. The comparison sequences are tighter around the usual brightness of the symbiotic stars and become looser away from it. In most cases the sequences extend to much fainter magnitudes (down to  $B \geq 19$  mag or  $B \geq 20$  mag) than reached

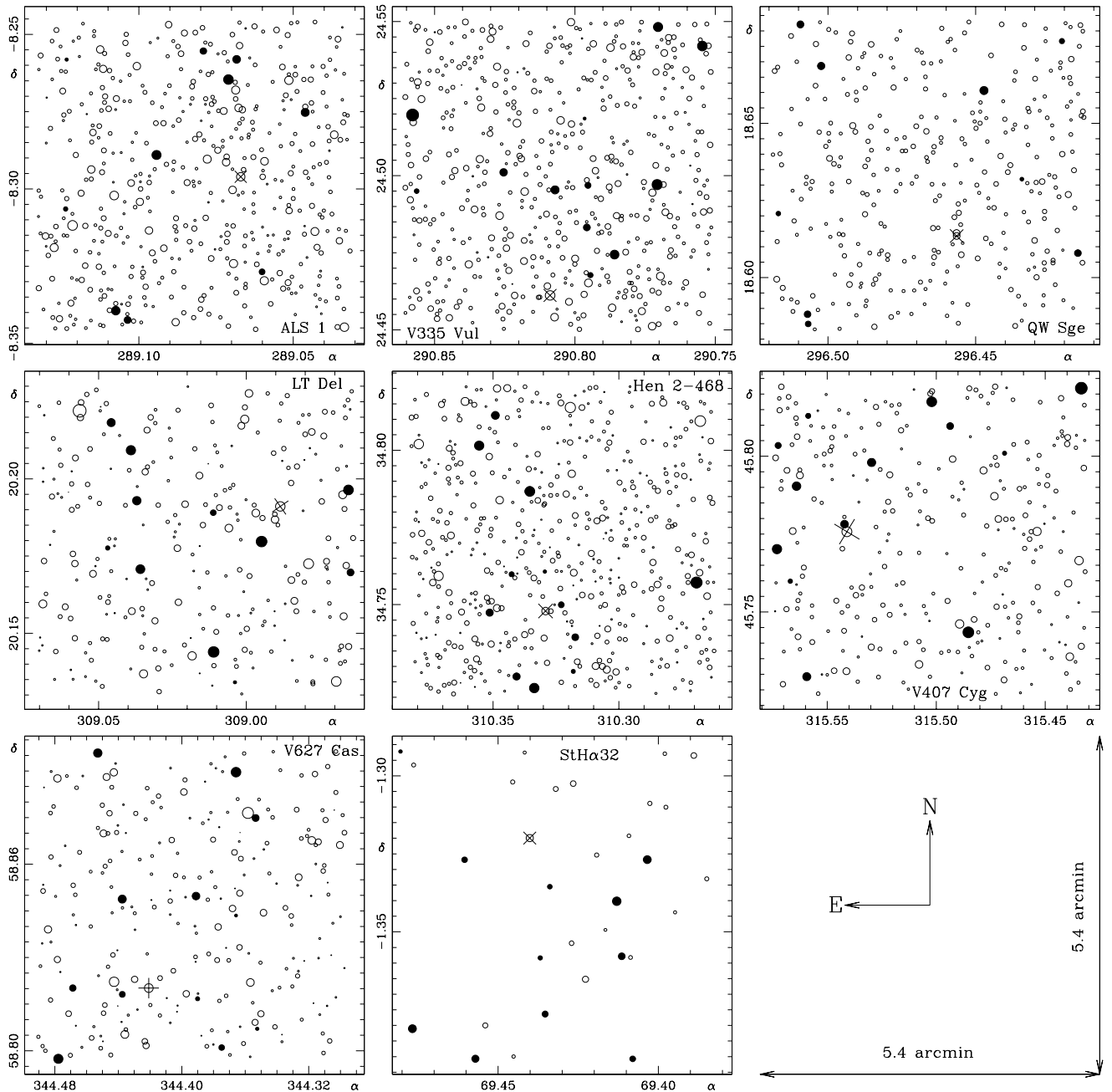


Fig. 2. Same as Fig. 1

by the respective symbiotic stars because they could be of interest to other observational projects as well as in assisting in the calibration of sky survey projects on photographic plates.

For 9 objects (Draco C-1, ALS 2, K 3-9, V919 Sgr, Ap 3-1, V335 Vul, Hen 3-468, V627 Cas and StH $\alpha$  32) the symbiotic star and the comparison sequence both lie inside a  $5.16 \times 5.16$  arcmin field (see Fig. 1), which match in dimension the Allen (1984) finding charts. For the remaining 11 program objects, comparison stars bright enough to cover the outburst phases had to be found at greater distance from the symbiotic star. They are given in Table 2

at the end of each sequence, separated by an empty line from the other comparison stars, and are plotted on the less deep and wider finding charts of Fig. 3.

The stars included in the comparison sequences have been checked on at least three different nights for variability (see Col. *N* of Table 2). We cannot rule out beyond doubt that some of them are indeed variable (they could be eclipsing systems observed outside eclipse, for example), but the fairly good agreement (at a few millimag level) of their magnitudes as measured on different nights over some months gives some confidence in their use. Finally, to avoid problems of blending with nearby

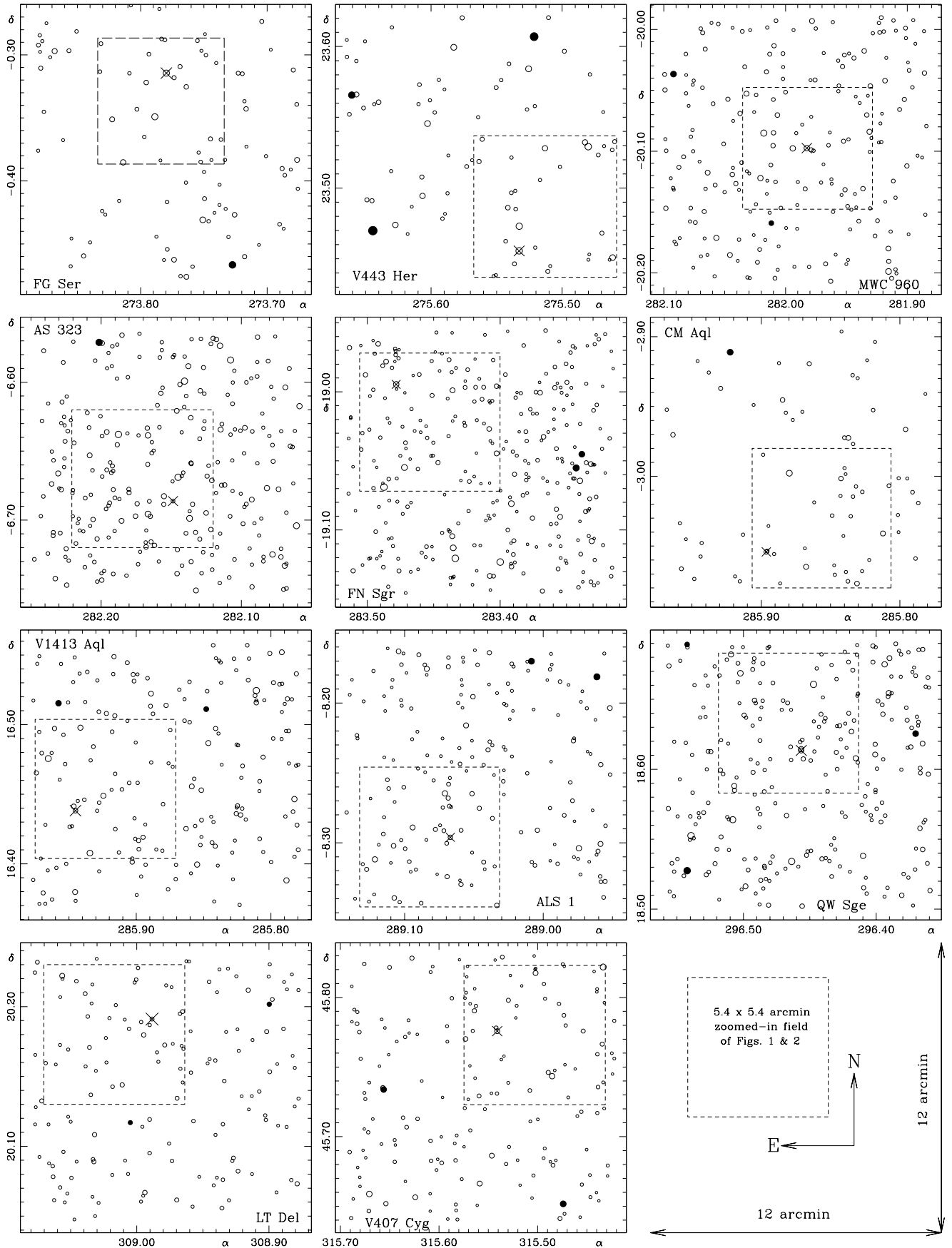


**Fig. 3.** Comparison stars bright enough to cover the outburst phases lay outside the fields of Figs. 1 and 2 for eleven symbiotic stars. They are identified in these wider finding charts, where the portion plotted in greater detail in Figs. 1 and 2 is outlined by a dashed square. The symbols are the same as in Figs. 1 and 2, with an imaged field of view of about  $11.4 \times 11.4$  arcmin and a  $12 \times 12$  arcmin coordinate grid. To avoid overcrowding, the limiting magnitude is much brighter ( $V \sim 16$  mag) than in Figs. 1 and 2

stars on plates or CCD images from short focus telescopes, the comparison stars have been selected so as to avoid those with close companions.

#### 4. The type of variability in symbiotic stars

As a guideline for observers not familiar with the symbiotic stars, a few simplified notes may be of interest concerning the types of variability one may expect from the latter and the best way to observe them. We will limit the discussion to the photometric bands of the  $UBV(RI)_C$  system.

The variability ascribed to the *cool giant* is best observed at longer wavelengths (i.e. the  $I$  band. The  $R$  band is affected by the usually very strong  $H\alpha$  emission), where the contamination from the white dwarf companion and the circumstellar material become less important. Basically, two types of variability of the cool giant may be observed:

*intrinsic*, like the pulsations of a Mira variable (about  $\sim 20\%$  of the known symbiotics harbor a Mira). The amplitude of variability generally decreases toward longer wavelengths. Popular examples are R Aqr (pulsation period of 386 days, minima as faint as  $V = 12$ , maxima as bright as  $V = 5$  mag) or UV Aur (pulsation period of 395 days, minima as faint as  $V = 11$ , maxima as bright as  $V = 7.5$  mag);

*ellipsoidal*, when the cool giant fills its Roche lobe. Due to the orbital motion the area of the Roche lobe projected onto the sky varies continuously, with two maxima (when the binary system is seen at quadrature) and two minima (when the cool giant passes at superior or inferior conjunctions) per orbital cycle. Because the reason for variability is a geometrical one, the amplitude of variability is not strongly dependent upon wavelength. Popular examples of symbiotic stars showing ellipsoidal distortion of their lightcurve are T CrB (orbital period 227 days, amplitude  $\Delta m = 0.3$  mag) and BD-21.3873 (orbital period 285 days, amplitude  $\Delta m = 0.2$  mag).

The variability ascribed to the *hot white dwarf* companion to the cool giant is best observed at shorter wavelengths. There are several type of manifestations, among which:

*outbursts*, with amplitudes  $\Delta B = 2 - 5$  mag and duration from half a year to many decades. The amplitude, duration and lightcurve shape are usually unpredictable. The same system might show completely different type of outbursts one after the other. For example, QW Sge had an outburst extending from July 1962 to March 1972 characterized by a rapid rise and a linear and smooth decline, followed by another one from May 1982 to September 1989 showing a complex lightcurve with more than one maximum and deep minima in between;

*reflection effect*, when the hard radiation field of the hot and luminous white dwarf (radiating mainly in the X-ray

and far ultraviolet domains) illuminates and heats up the facing side of the cool giant (which reprocesses to the optical domain the energy received by the white dwarf). The heated side of the cool giant is therefore a bit brighter and bluer than the opposite one (which is not illuminated by the white dwarf radiation field). During an orbital period the heated side comes and goes from view, causing a sinusoidal lightcurve. The effect is strongly wavelength dependent, being maximum in the  $U$  band and undetectable in  $R$  and  $I$  bands. The amplitude may be fairly large, as in LT Del where  $\Delta U = 1.6$ ,  $\Delta B = 0.5$  and  $\Delta V = 0.2$  mag. It should be observable in the majority of symbiotic stars (more and more easily as the white dwarf gets hotter and the orbital inclination increases) and it is a powerful way to measure orbital periods;

*eclipses* of the white dwarf by the cool giant. In quiescence the eclipses generally escape detection by optical photometry because the white dwarf is radiating mostly at shorter wavelengths (X-rays and far ultraviolet). During the outbursts the white dwarf emission shifts to longer wavelengths and becomes conspicuous in the optical, thus allowing the eclipses to be detected if the orbital inclination is sufficiently high. Classical examples of symbiotic stars for which the eclipses passed undetected in quiescence and instead became outstanding features of the outburst lightcurve are FG Ser and V1413 Aql. Because the eclipsing body is cool and the eclipsed one is hot, the visibility of eclipses increases toward shorter wavelengths (for example for FG Ser in outburst it was  $\Delta V = 1.4$ ,  $\Delta B = 1.9$  and  $\Delta U = 2.3$  mag);

*re-processing* by the circumstellar nebula of the energy radiated by the white dwarf. Sometimes there is so much circumstellar gas ionized by the radiation field of the white dwarf that its brightness completely overwhelms that of the binary system, as it is for the popular cases of V1016 Cyg and V852 Cen (the *Southern Crab*). Both these symbiotic binaries harbor a Mira variable, whose variability however does not at all affect the optical photometry because of the immensely brighter circumstellar ionized gas. When the white dwarf becomes progressively cooler and dimmer, the amount of ionizing photons that it releases goes down, and the ionized fraction of the circumstellar nebula decreases and consequently its brightness (the scenario is valid for radiation bounded nebulae). This is the case for HM Sge that over the last 25 years has gradually become fainter by  $\Delta V = 0.031$  and  $\Delta B = 0.086$  mag yr $^{-1}$ .

#### 5. Notes on individual symbiotic stars

A few individual notes follow on the photometric behavior of the program symbiotic stars, to the aim of assisting the interested reader in planning an observing strategy. An inspiring reading would also be the collected history of symbiotic stars assembled by Kenyon (1986).

**Table 2.** The comparison sequences around the 20 program symbiotic stars. Positions for J2000 equinox and a mean epoch 1999.5 are given (errors in arcsec are derived from different exposures in different bands), together with magnitudes and colors (errors in magnitudes). The stars in each sequence are ordered according to fainter  $B$  magnitudes.  $N$  is the number of observing nights. The sequences are given in the same order as in Table 1 and Figs. 1 and 2. The comparison stars laying outside the field of view of Figs. 1 and 2 and plotted in Fig. 3 are given at the bottom of each sequence, separated by an empty line

$\alpha_{J2000}$ ( $\pm''$ )	$\delta_{J2000}$ ( $\pm''$ )	$N$	$B$ ( $\pm$ )	$V$ ( $\pm$ )	$B-V$ ( $\pm$ )	$U-B$ ( $\pm$ )	$V-R_C$ ( $\pm$ )	$R-I_C$ ( $\pm$ )		
<b>Draco C-1</b>										
260.072449	0.008	57.871140	0.005	3	14.767 0.010	14.123 0.008	0.644 0.006	0.094 0.040	0.370 0.008	0.371 0.016
259.947144	0.008	57.872383	0.007	3	15.264 0.008	14.349 0.005	0.915 0.006	0.651 0.034	0.531 0.009	0.468 0.008
259.928192	0.037	57.796032	0.030	3	15.834 0.007	15.233 0.006	0.601 0.004	0.027 0.045	0.366 0.008	0.320 0.012
260.032379	0.000	57.812370	0.004	3	16.328 0.008	15.363 0.006	0.965 0.005	0.620 0.034	0.517 0.007	0.481 0.005
260.077576	0.030	57.855206	0.037	3	16.942 0.011	16.369 0.009	0.573 0.006	-0.073 0.043	0.333 0.012	0.335 0.008
259.894043	0.008	57.841286	0.006	3	17.711 0.013	16.704 0.006	1.007 0.012	0.856 0.065	0.643 0.007	0.519 0.013
259.982147	0.000	57.814522	0.011	3	18.238 0.016	17.447 0.013	0.791 0.010	0.298 0.035	0.465 0.009	0.430 0.010
259.901337	0.045	57.856976	0.051	3	18.589 0.023	17.329 0.006	1.260 0.022		0.701 0.007	0.619 0.009
259.971069	0.012	57.860584	0.022	3	18.981 0.019	17.974 0.009	1.007 0.017	0.309 0.077	0.585 0.016	0.581 0.013
259.987640	0.028	57.882824	0.010	3	19.425 0.021	18.631 0.009	0.794 0.019	0.279 0.101	0.525 0.019	0.496 0.039
260.011536	0.094	57.815956	0.050	3	20.123 0.078	19.339 0.019	0.784 0.083	0.114 0.157	0.445 0.056	0.569 0.070
260.021545	0.092	57.830807	0.073	3	20.587 0.085	19.787 0.047	0.800 0.062		0.407 0.144	0.643 0.171
<b>ALS 2</b>										
267.734589	0.136	-17.738707	0.025	3	12.856 0.030	12.421 0.014	0.435 0.026	0.320 0.054	0.270 0.020	0.304 0.010
267.740845	0.102	-17.761610	0.040	3	14.103 0.029	13.187 0.023	0.916 0.018	0.392 0.049	0.611 0.025	0.601 0.009
267.728668	0.124	-17.740768	0.040	3	14.442 0.019	13.638 0.011	0.804 0.016	0.335 0.040	0.502 0.034	0.514 0.017
267.679626	0.043	-17.744520	0.054	3	15.048 0.021	13.406 0.014	1.642 0.016	1.698 0.053	0.951 0.027	0.839 0.007
267.746094	0.076	-17.777182	0.036	2	15.647 0.029	14.153 0.023	1.494 0.017	1.241 0.010	0.881 0.030	0.781 0.017
267.661560	0.075	-17.805332	0.088	3	16.018 0.021	15.209 0.017	0.809 0.012	0.369 0.048	0.545 0.032	0.501 0.022
267.738129	0.015	-17.799183	0.109	3	16.422 0.016	14.811 0.005	1.611 0.015	1.661 0.010	0.971 0.022	0.859 0.007
267.680847	0.072	-17.757969	0.029	3	17.003 0.022	15.941 0.017	1.062 0.014	0.556 0.080	0.664 0.016	0.602 0.040
267.725006	0.078	-17.802011	0.100	3	17.572 0.028	15.551 0.018	2.021 0.021		1.694 0.007	1.897 0.032
267.660370	0.048	-17.822681	0.120	3	18.039 0.036	16.311 0.018	1.728 0.031		1.023 0.019	0.890 0.019
267.678009	0.101	-17.740681	0.068	3	18.481 0.031	17.057 0.011	1.424 0.029		0.959 0.023	0.808 0.022
267.701721	0.050	-17.743387	0.122	3	19.010 0.059	17.463 0.048	1.547 0.034		0.902 0.090	0.780 0.043
<b>FG Ser</b>										
273.788727	0.064	-0.349092	0.035	5	12.537 0.026	11.811 0.018	0.726 0.019	0.194 0.043	0.439 0.007	0.442 0.009
273.813843	0.061	-0.385280	0.026	5	13.940 0.026	12.825 0.016	1.115 0.020	1.052 0.069	0.685 0.009	0.569 0.008
273.822510	0.096	-0.351158	0.019	5	14.242 0.025	13.296 0.016	0.946 0.019	0.335 0.045	0.589 0.012	0.594 0.009
273.763947	0.046	-0.325394	0.029	5	14.732 0.028	13.820 0.018	0.912 0.021	0.491 0.040	0.553 0.011	0.587 0.012
273.831329	0.128	-0.291071	0.046	4	15.598 0.044	14.823 0.036	0.775 0.026	0.283 0.035	0.472 0.016	0.551 0.023
273.752502	0.027	-0.384941	0.042	5	16.197 0.033	15.004 0.016	1.193 0.029	0.551 0.073	0.745 0.013	0.746 0.016
273.793457	0.048	-0.299392	0.024	5	16.975 0.042	14.742 0.019	2.233 0.038	2.383 0.043	1.316 0.017	1.269 0.008
273.765411	0.027	-0.343956	0.049	5	17.860 0.044	16.735 0.022	1.125 0.038	0.280 0.146	0.709 0.034	0.740 0.037
273.805176	0.058	-0.341544	0.059	5	18.481 0.056	16.941 0.015	1.540 0.054		1.078 0.011	1.243 0.033
273.764343	0.139	-0.372931	0.074	4	19.248 0.099	17.819 0.028	1.429 0.095		0.941 0.025	0.944 0.102
<b>V443 Her</b>										
275.480103	0.015	23.529230	0.023	3	12.113 0.008	11.399 0.008	0.714 0.001	0.213 0.022	0.425 0.001	0.376 0.009
275.532715	0.025	23.473034	0.012	3	12.726 0.009	11.547 0.009	1.179 0.002	1.167 0.018	0.650 0.008	0.527 0.005
275.461517	0.025	23.450865	0.029	3	13.388 0.009	12.411 0.005	0.977 0.007	0.669 0.027	0.576 0.003	0.488 0.011
275.482574	0.015	23.532297	0.022	3	13.720 0.010	12.907 0.000	0.813 0.010	0.370 0.020	0.473 0.004	0.412 0.016
275.513092	0.015	23.528137	0.011	3	14.367 0.008	12.986 0.006	1.381 0.005	1.539 0.069	0.752 0.011	0.634 0.020
275.510925	0.015	23.441086	0.015	3	15.006 0.010	14.249 0.006	0.757 0.008	0.244 0.034	0.434 0.016	0.376 0.017
275.538757	0.029	23.496637	0.033	3	15.547 0.011	14.901 0.008	0.646 0.007	0.073 0.044	0.418 0.009	0.345 0.012
275.516907	0.015	23.505695	0.068	3	16.427 0.015	15.350 0.009	1.077 0.012	0.961 0.018	0.621 0.020	0.481 0.011
<b>K 3-9</b>										
275.644470	0.063	23.469881	0.099	3	9.400 0.103	8.899 0.100	0.501 0.025	-0.308 0.041	0.208 0.078	0.124 0.044
275.521393	0.015	23.606977	0.022	3	11.395 0.025	9.710 0.018	1.685 0.018	2.105 0.021	0.937 0.015	0.902 0.009
275.660553	0.029	23.565674	0.037	3	11.889 0.006	11.354 0.005	0.535 0.003	0.021 0.030	0.317 0.006	0.316 0.017
<b>K 3-9</b>										
280.101990	0.145	-8.698515	0.204	3	14.237 0.019	13.499 0.016	0.738 0.010	0.339 0.048	0.486 0.022	0.536 0.009
280.145325	0.093	-8.723275	0.158	3	15.390 0.032	14.457 0.027	0.933 0.017	0.504 0.048	0.606 0.015	0.639 0.010
280.157623	0.000	-8.758720	0.100	3	15.668 0.051	13.298 0.050	2.370 0.012	2.638 0.030	1.428 0.053	1.556 0.076
280.128906	0.022	-8.776566	0.042	3	16.324 0.027	15.286 0.022	1.038 0.015	0.410 0.051	0.649 0.013	0.657 0.013
280.091034	0.059	-8.751462	0.100	3	16.985 0.030	15.970 0.016	1.015 0.025	0.592 0.038	0.657 0.011	0.688 0.008
280.131866	0.041	-8.750023	0.121	3	17.576 0.016	16.266 0.016	1.310 0.003	0.699 0.025	0.842 0.008	0.841 0.011
280.131744	0.090	-8.709950	0.159	3	17.857 0.037	16.589 0.031	1.268 0.020	0.553 0.046	0.843 0.043	0.955 0.086
280.093201	0.047	-8.755725	0.090	3	18.435 0.039	17.241 0.018	1.194 0.035	0.594 0.071	0.779 0.016	0.803 0.056
280.074097	0.047	-8.777774	0.042	3	18.823 0.051	17.639 0.041	1.184 0.030	0.493 0.024	0.782 0.026	0.853 0.008
280.125641	0.151	-8.714624	0.198	4	19.266 0.053	17.909 0.029	1.357 0.044	0.696 0.058	0.891 0.025	0.917 0.014
280.130768	0.078	-8.714277	0.165	3	19.691 0.050	18.091 0.048	1.600 0.014		1.028 0.049	1.030 0.012
280.143005	0.065	-8.757268	0.129	3	20.014 0.093	18.330 0.085	1.684 0.037		1.018 0.016	1.019 0.072

Table 2. continued

$\alpha_{J2000}$ ( $\pm''$ )	$\delta_{J2000}$ ( $\pm''$ )	N	$B$ ( $\pm$ )	$V$ ( $\pm$ )	$B-V$ ( $\pm$ )	$U-B$ ( $\pm$ )	$V-R_C$ ( $\pm$ )	$R-I_C$ ( $\pm$ )								
<b>MWC 960</b>																
282.017883	0.040	-20.085129	0.081	5	12.429	0.031	11.322	0.026	1.107	0.017	0.787	0.018	0.590	0.037	0.564	0.023
281.994141	0.057	-20.097675	0.032	5	12.911	0.037	12.235	0.035	0.676	0.011	0.134	0.010	0.390	0.041	0.397	0.027
282.032104	0.064	-20.052744	0.119	5	13.490	0.041	12.811	0.039	0.679	0.013	0.160	0.020	0.388	0.039	0.400	0.023
282.006714	0.038	-20.070320	0.070	5	13.729	0.040	13.234	0.037	0.495	0.016	0.245	0.015	0.264	0.032	0.266	0.035
281.931061	0.059	-20.084045	0.088	5	13.895	0.034	12.565	0.031	1.330	0.013	1.304	0.020	0.704	0.042	0.598	0.032
281.952393	0.068	-20.091818	0.071	5	14.598	0.037	13.821	0.036	0.777	0.010	0.221	0.016	0.450	0.045	0.425	0.028
282.009888	0.055	-20.084902	0.070	5	15.143	0.041	13.474	0.033	1.669	0.024	1.977	0.011	0.919	0.039	0.835	0.022
281.949005	0.202	-20.145264	0.056	6	15.719	0.031	14.368	0.028	1.351	0.014	1.375	0.045	0.736	0.058	0.652	0.025
282.015350	0.070	-20.135010	0.098	5	16.380	0.032	15.499	0.031	0.881	0.008	0.438	0.060	0.490	0.051	0.443	0.011
281.970703	0.020	-20.048611	0.053	5	17.022	0.042	15.544	0.039	1.478	0.016	1.521	0.057	0.827	0.023	0.771	0.024
282.033508	0.070	-20.075802	0.118	5	17.695	0.101	16.686	0.041	1.009	0.092	0.591	0.018	0.565	0.021	0.561	0.042
281.964447	0.030	-20.057562	0.046	4	18.082	0.046	16.604	0.024	1.478	0.039			0.801	0.013	0.705	0.033
281.969818	0.166	-20.118492	0.123	3	19.097	0.083	17.905	0.061	1.192	0.057			0.667	0.095	0.477	0.096
282.092072	0.144	-20.036648	0.317	3	13.061	0.035	11.733	0.024	1.328	0.025	1.205	0.025	0.696	0.037	0.638	0.029
282.011719	0.084	-20.159088	0.102	5	13.594	0.045	13.003	0.044	0.591	0.008	0.230	0.018	0.333	0.041	0.359	0.035
<b>AS 323</b>																
282.155182	0.239	-6.682678	0.145	3	12.942	0.022	12.571	0.008	0.371	0.020	0.203	0.039	0.202	0.030	0.227	0.024
282.166595	0.239	-6.638593	0.149	3	13.424	0.049	12.165	0.026	1.259	0.041	0.977	0.045	0.706	0.031	0.660	0.011
282.146027	0.145	-6.620771	0.138	3	13.926	0.020	12.949	0.006	0.977	0.019	0.569	0.044	0.592	0.025	0.562	0.019
282.202820	0.485	-6.713652	0.216	3	14.480	0.040	13.594	0.025	0.886	0.031	0.406	0.049	0.495	0.029	0.464	0.025
282.163849	0.242	-6.651345	0.154	3	14.980	0.019	14.144	0.009	0.836	0.017	0.358	0.029	0.486	0.024	0.457	0.017
282.196442	0.434	-6.691963	0.196	3	15.374	0.029	14.509	0.011	0.865	0.027	0.355	0.036	0.494	0.034	0.468	0.019
282.168152	0.322	-6.716187	0.184	3	15.689	0.026	14.815	0.012	0.874	0.023	0.241	0.020	0.514	0.030	0.503	0.012
282.160095	0.235	-6.667989	0.139	3	16.155	0.022	15.374	0.000	0.781	0.022	0.365	0.071	0.457	0.033	0.439	0.016
282.164703	0.270	-6.693072	0.126	3	16.590	0.030	15.670	0.017	0.920	0.025	0.518	0.064	0.571	0.006	0.472	0.032
282.191193	0.415	-6.694499	0.198	3	17.118	0.030	16.182	0.022	0.936	0.020	0.369	0.047	0.540	0.053	0.563	0.021
282.180511	0.366	-6.683941	0.220	3	17.715	0.076	16.724	0.056	0.991	0.052	0.507	0.096	0.628	0.036	0.670	0.034
282.157715	0.255	-6.667590	0.146	3	18.680	0.030	17.570	0.014	1.110	0.026	0.475	0.016	0.706	0.017	0.535	0.039
282.201385	0.000	-6.571096	0.326	2	11.286	0.084	10.961	0.083	0.325	0.014	-0.332	0.093	0.339	0.006	0.225	0.024
<b>FN Sgr</b>																
283.472046	0.091	-19.054768	0.047	3	12.895	0.014	11.699	0.000	1.196	0.013	1.142	0.018	0.663	0.008	0.599	0.007
283.435822	0.087	-18.998878	0.155	3	13.328	0.012	12.840	0.006	0.488	0.010	0.092	0.013	0.305	0.012	0.304	0.006
283.501404	0.224	-18.987713	0.759	5	13.911	0.031	13.478	0.027	0.433	0.015	0.141	0.008	0.277	0.012	0.292	0.008
283.402649	0.104	-19.044584	0.067	3	14.338	0.013	12.788	0.000	1.550	0.013	1.863	0.027	0.884	0.011	0.819	0.010
283.451233	0.088	-19.002655	0.167	3	15.033	0.014	13.848	0.009	1.185	0.011	1.065	0.020	0.647	0.017	0.592	0.010
283.488464	0.076	-18.981091	0.176	3	15.427	0.018	14.115	0.014	1.312	0.012	1.352	0.008	0.740	0.018	0.674	0.005
283.494385	0.083	-18.972382	0.195	3	15.804	0.026	14.834	0.024	0.970	0.011	0.578	0.008	0.562	0.013	0.544	0.005
283.439484	0.092	-19.004942	0.171	3	16.563	0.010	15.230	0.009	1.333	0.005	1.443	0.079	0.726	0.014	0.630	0.016
283.498932	0.067	-19.040255	0.076	3	17.708	0.035	16.928	0.026	0.780	0.023	0.269	0.027	0.455	0.016	0.505	0.028
283.463013	0.097	-18.995384	0.230	3	18.548	0.056	17.670	0.051	0.878	0.024			0.496	0.070	0.390	0.084
283.342773	0.113	-19.055079	0.082	3	11.682	0.076	11.162	0.063	0.520	0.043	-0.032	0.110	0.380	0.054	0.299	0.011
283.338531	0.117	-19.045137	0.095	3	12.519	0.008	11.766	0.005	0.753	0.006	0.360	0.022	0.441	0.003	0.378	0.005
<b>V919 Sgr</b>																
285.893860	0.034	-16.952595	0.029	3	12.466	0.109	10.776	0.086	1.690	0.067	2.140	0.057	1.082	0.027	1.038	0.048
285.971039	0.057	-17.012613	0.025	3	12.627	0.025	12.123	0.021	0.504	0.013	0.184	0.034	0.298	0.003	0.304	0.007
285.922089	0.043	-16.998413	0.008	3	13.536	0.029	12.944	0.014	0.592	0.025	0.057	0.015	0.368	0.004	0.364	0.004
285.970551	0.040	-16.997137	0.011	3	13.856	0.034	13.145	0.020	0.711	0.027	0.203	0.016	0.420	0.002	0.402	0.009
285.953613	0.071	-16.935564	0.038	3	14.289	0.028	12.616	0.020	1.673	0.020	1.829	0.009	1.170	0.001	1.459	0.016
285.967102	0.040	-16.996569	0.011	3	14.744	0.025	13.568	0.015	1.176	0.020	0.999	0.028	0.654	0.005	0.610	0.007
285.954712	0.061	-17.014524	0.012	3	15.208	0.026	14.080	0.008	1.128	0.025	0.842	0.027	0.641	0.006	0.601	0.008
285.923767	0.030	-16.989100	0.004	3	15.874	0.023	14.663	0.015	1.211	0.018	1.068	0.014	0.674	0.006	0.598	0.006
285.879883	0.015	-16.965837	0.030	3	16.440	0.028	15.318	0.009	1.122	0.027	0.893	0.038	0.659	0.012	0.587	0.015
285.958038	0.015	-16.977039	0.051	3	17.030	0.036	16.258	0.021	0.772	0.029	0.294	0.053	0.451	0.032	0.432	0.052
285.972443	0.050	-16.941414	0.031	3	18.136	0.034	17.135	0.016	1.001	0.030	0.572	0.049	0.598	0.028	0.563	0.026
285.875580	0.057	-16.945108	0.158	3	19.198	0.078	18.235	0.035	0.963	0.070	0.416	0.057	0.467	0.017	0.519	0.062
<b>CM Aql</b>																
285.812164	0.016	-3.040951	0.015	3	13.609	0.012	12.719	0.006	0.890	0.010	0.400	0.031	0.510	0.007	0.483	0.001
285.879761	0.103	-2.997757	0.072	3	13.955	0.089	11.702	0.067	2.253	0.058	2.653	0.067	1.242	0.023	1.470	0.019
285.842438	0.027	-3.001642	0.014	3	14.243	0.016	13.421	0.005	0.822	0.015	0.458	0.024	0.471	0.005	0.544	0.010
285.830933	0.039	-3.076826	0.047	3	14.941	0.021	13.134	0.013	1.807	0.017	1.816	0.030	0.975	0.007	0.916	0.007
285.848877	0.042	-3.028200	0.033	3	15.273	0.020	14.391	0.013	0.882	0.015	0.531	0.023	0.496	0.008	0.572	0.018
285.827087	0.016	-3.011171	0.004	3	15.828	0.017	14.509	0.008	1.319	0.015	0.765	0.033	0.779	0.007	0.763	0.007
285.839935	0.000	-2.994117	0.015	3	16.286	0.028	15.022	0.022	1.264	0.017	0.578	0.067	0.759	0.008	0.753	0.004
285.820312	0.027	-2.996999	0.025	3	17.250	0.021	15.579	0.013	1.671	0.016	1.147	0.065	0.977	0.012	0.957	0.009
285.834686	0.016	-3.075637	0.060	3	18.276	0.019	17.321	0.017	0.955	0.008	0.577	0.071	0.559	0.046	0.609	0.050
285.885132	0.117	-3.008897	0.087	3	19.102	0.038	17.790	0.006	1.312	0.038	0.773	0.018	0.751	0.041	0.796	0.112
285.855621	0.073	-3.057502	0.130	3	20.009	0.087	17.934	0.038	2.075	0.078			1.159	0.059	1.065	0.020
285.922424	0.146	-2.911115	0.113	3	12.306	0.056	11.651	0.052	0.655	0.022	0.216	0.059	0.493	0.043	0.389	0.012



Table 2. continued

$\alpha_{J2000}$ ( $\pm''$ )	$\delta_{J2000}$ ( $\pm''$ )	N	$B$ ( $\pm$ )	$V$ ( $\pm$ )	$B-V$ ( $\pm$ )	$U-B$ ( $\pm$ )	$V-R_c$ ( $\pm$ )	$R-I_c$ ( $\pm$ )		
<b>LT Del</b>										
309.011017	0.021	20.143934	0.022	3	13.179 0.010	12.155 0.010	1.024 0 .003	0.746 0.023	0.538 0.002	0.508 0.007
308.965363	0.026	20.196424	0.004	3	13.431 0.007	12.895 0.005	0.536 0 .005	0.082 0.023	0.316 0.007	0.298 0.013
308.994781	0.015	20.179708	0.007	3	13.871 0.009	12.210 0.005	1.661 0 .008	2.069 0.001	0.933 0.001	0.975 0.006
309.039032	0.033	20.209257	0.017	3	14.273 0.008	13.223 0.005	1.050 0 .006	0.819 0.019	0.552 0.003	0.518 0.012
309.035828	0.026	20.170765	0.015	3	14.401 0.011	13.569 0.010	0.832 0 .004	0.419 0.015	0.448 0.002	0.428 0.007
309.037109	0.026	20.192942	0.007	3	14.930 0.009	13.936 0.008	0.994 0 .003	0.611 0.026	0.546 0.003	0.539 0.002
309.045654	0.033	20.218222	0.022	3	15.496 0.011	14.173 0.008	1.323 0 .008	1.482 0.021	0.702 0.003	0.628 0.005
308.964661	0.021	20.169697	0.019	3	15.949 0.006	15.143 0.000	0.806 0 .006	0.510 0.019	0.436 0.008	0.373 0.010
309.011139	0.021	20.189051	0.014	3	16.858 0.009	16.082 0.006	0.776 0 .007	0.200 0.047	0.457 0.020	0.576 0.018
309.046906	0.052	20.177620	0.037	3	18.052 0.022	17.142 0.019	0.910 0 .011	0.541 0.055	0.479 0.039	0.491 0.084
309.003876	0.056	20.134117	0.101	3	19.335 0.014	18.022 0.000	1.313 0 .014		0.814 0.011	0.827 0.074
308.899841	0.026	20.201719	0.004	3	12.350 0.035	11.831 0.035	0.519 0 .002	0.057 0.025	0.316 0.007	0.285 0.006
309.004944	0.036	20.116964	0.030	3	12.893 0.008	12.366 0.008	0.527 0 .002	0.050 0.023	0.296 0.001	0.304 0.006
<b>Hen 2-468</b>										
310.269104	0.018	34.757172	0.008	3	12.896 0.042	11.632 0.023	1.264 0.035	1.092 0.045	0.932 0.183	
310.335388	0.047	34.786682	0.011	3	13.510 0.006	12.782 0.005	0.728 0.003	0.256 0.016	0.402 0.001	0.394 0.002
310.355560	0.023	34.801491	0.005	3	13.838 0.005	13.289 0.005	0.549 0.001	-0.009 0.016	0.318 0.000	0.334 0.009
310.333649	0.023	34.723000	0.017	3	14.799 0.005	13.092 0.005	1.707 0.001	1.698 0.008	0.950 0.006	0.891 0.007
310.349060	0.029	34.811295	0.005	3	15.426 0.008	14.486 0.006	0.940 0.005	0.705 0.003	0.533 0.011	0.484 0.005
310.351379	0.026	34.747395	0.003	3	16.025 0.007	15.108 0.006	0.917 0.004	0.263 0.007	0.555 0.007	0.563 0.003
310.317291	0.000	34.739445	0.015	3	16.546 0.006	15.528 0.000	1.018 0.006	0.457 0.010	0.608 0.002	0.615 0.010
310.340637	0.013	34.726719	0.015	3	16.900 0.006	15.115 0.000	1.785 0.006	1.858 0.009	1.016 0.009	0.964 0.008
310.322937	0.000	34.749947	0.008	3	17.468 0.011	16.335 0.006	1.133 0.009	1.018 0.021	0.667 0.004	0.597 0.003
310.342590	0.034	34.759830	0.011	3	18.108 0.010	16.997 0.009	1.111 0.005	0.629 0.040	0.640 0.013	0.620 0.015
310.318146	0.029	34.728374	0.098	3	19.057 0.022	17.884 0.009	1.173 0.020	0.527 0.074	0.726 0.012	0.660 0.053
310.329468	0.018	34.760708	0.055	3	20.072 0.050	18.509 0.026	1.563 0.043		1.016 0.005	1.050 0.071
<b>V407 Cyg</b>										
315.433502	0.019	45.821873	0.015	3	11.050 0.100	10.051 0.095	0.999 0.032	-0.203 0.040	0.636 0.091	0.337 0.006
315.485260	0.044	45.743469	0.042	3	11.484 0.050	10.951 0.013	0.533 0.048	-0.010 0.063	0.182 0.015	0.188 0.016
315.502075	0.019	45.817524	0.008	3	12.561 0.009	11.822 0.008	0.739 0.004	0.287 0.033	0.405 0.003	0.355 0.010
315.573059	0.041	45.770191	0.008	3	12.857 0.011	12.233 0.011	0.624 0.000	0.112 0.033	0.348 0.008	0.344 0.000
315.564117	0.048	45.790409	0.013	3	13.582 0.009	12.908 0.009	0.674 0.001	0.106 0.034	0.386 0.006	0.381 0.013
315.529633	0.016	45.798008	0.008	3	14.014 0.006	13.236 0.005	0.778 0.004	0.210 0.029	0.464 0.005	0.425 0.007
315.542023	0.000	45.778206	0.029	3	14.335 0.016	13.705 0.016	0.630 0.003	0.361 0.026	0.488 0.007	0.832 0.065
315.559418	0.000	45.729229	0.030	3	14.900 0.015	13.360 0.014	1.540 0.005	1.236 0.022	0.901 0.004	0.841 0.008
315.493622	0.000	45.809704	0.018	3	15.576 0.018	14.475 0.014	1.101 0.011	0.539 0.021	0.685 0.010	0.661 0.037
315.572510	0.049	45.803467	0.009	3	16.187 0.012	15.155 0.006	1.032 0.010	0.458 0.048	0.629 0.015	0.580 0.057
315.558777	0.058	45.812984	0.052	3	16.767 0.007	16.013 0.006	0.754 0.003	0.576 0.031	0.456 0.036	0.457 0.038
315.566956	0.011	45.759872	0.104	3	18.035 0.033	16.659 0.026	1.376 0.021	0.811 0.111	0.782 0.037	0.725 0.061
315.468658	0.019	45.800968	0.021	3	19.021 0.039	16.866 0.039	2.155 0.005		1.226 0.040	1.130 0.036
315.474060	0.134	45.651703	0.356	2	10.767 0.115	10.121 0.113	0.646 0.021	-0.491 0.043	0.219 0.116	0.031 0.021
315.656128	0.048	45.733856	0.014	3	11.704 0.062	10.478 0.061	1.226 0.010	0.922 0.036	0.694 0.055	0.587 0.009
<b>V627 Cas</b>										
344.365906	0.031	58.889633	0.026	3	12.493 0.029	11.966 0.005	0.527 0.029	0.017 0.035	0.262 0.006	0.271 0.009
344.477783	0.097	58.797409	0.119	3	12.844 0.004	12.323 0.000	0.521 0.004	0.119 0.012	0.300 0.004	0.323 0.010
344.452972	0.091	58.895763	0.040	3	13.648 0.007	13.072 0.005	0.576 0.005	0.363 0.010	0.326 0.007	0.373 0.010
344.437592	0.062	58.848778	0.073	3	14.023 0.009	13.358 0.008	0.665 0.003	0.360 0.006	0.387 0.006	0.429 0.013
344.391052	0.038	58.849773	0.042	3	14.588 0.005	13.741 0.005	0.847 0.001	0.279 0.008	0.522 0.008	0.540 0.007
344.353577	0.012	58.874886	0.033	3	15.034 0.010	14.354 0.000	0.680 0.010	0.179 0.041	0.450 0.007	0.472 0.009
344.468689	0.104	58.820171	0.092	3	15.743 0.008	14.801 0.006	0.942 0.006	0.361 0.010	0.561 0.002	0.556 0.016
344.437531	0.081	58.818161	0.094	3	16.245 0.009	15.292 0.006	0.953 0.007	0.035 0.011	0.618 0.010	0.651 0.035
344.374939	0.039	58.801048	0.098	3	16.727 0.010	15.539 0.009	1.188 0.004	1.049 0.003	0.705 0.022	0.644 0.050
344.390076	0.026	58.816742	0.019	3	17.891 0.015	16.848 0.013	1.043 0.007	0.386 0.022	0.657 0.028	0.661 0.024
344.352509	0.052	58.807072	0.098	3	18.763 0.010	17.555 0.006	1.208 0.008	0.678 0.073	0.761 0.056	0.636 0.077
344.365906	0.033	58.843506	0.046	3	19.503 0.060	17.935 0.027	1.568 0.054		1.013 0.040	0.993 0.020
<b>StH<math>\alpha</math> 32</b>										
69.412964	0.040	-1.340191	0.011	3	11.553 0.012	10.932 0.012	0.621 0.002	0.135 0.011	0.333 0.005	0.326 0.020
69.403458	0.042	-1.326853	0.011	3	12.410 0.010	11.852 0.010	0.558 0.003	-0.011 0.013	0.320 0.006	0.319 0.013
69.476753	0.021	-1.381033	0.027	3	12.746 0.013	11.795 0.013	0.951 0.001	0.691 0.016	0.503 0.005	0.471 0.018
69.457077	0.015	-1.390665	0.029	3	13.539 0.009	12.893 0.008	0.646 0.003	-0.002 0.008	0.343 0.008	0.350 0.023
69.411430	0.022	-1.357830	0.007	3	14.189 0.016	13.463 0.014	0.726 0.008	0.269 0.014	0.403 0.006	0.379 0.021
69.435333	0.033	-1.376335	0.027	3	15.110 0.016	14.483 0.014	0.627 0.008	0.048 0.023	0.356 0.006	0.367 0.037
69.407990	0.052	-1.390701	0.034	3	15.661 0.014	14.953 0.012	0.708 0.008	0.183 0.010	0.389 0.010	0.386 0.041
69.460472	0.032	-1.326894	0.012	3	16.561 0.008	15.081 0.000	1.480 0.008	1.099 0.081	0.982 0.013	1.164 0.007
69.433861	0.035	-1.335527	0.018	3	17.062 0.011	16.414 0.009	0.648 0.007	0.118 0.067	0.387 0.045	0.355 0.077
69.436859	0.026	-1.358345	0.098	3	17.925 0.021	16.877 0.017	1.048 0.012		0.572 0.023	0.558 0.100
69.480469	0.146	-1.292200	0.138	2	19.050 0.068	18.073 0.067	0.977 0.012		0.682 0.045	

While calibrating the photometric comparison sequences for this paper we have also collected data on the program symbiotic stars. These  $UBV(RI)_C$  data will be presented and discussed elsewhere together with similar data for more than another 100 symbiotic stars observed from ESO and Asiago. To the reader's benefit we report in this section mean  $B$  and  $B - V$  values for 1999 from the  $UBV(RI)_C$  survey (hereafter indicated as MHZ: Munari, Henden and Zwitter, in preparation).

**Draco C-1.** This carbon symbiotic star belongs to the Draco dwarf galaxy (Aaronson et al. 1982). Infrared photometry by Munari (1991a) proves C-1 to be at the tip of the Draco AGB with very blue IR colors for a carbon star, probably caused by the low metal content of the parent galaxy (Munari 1991b). No outburst has been so far recorded and the orbital period is unknown.  $BVI$  photometry by Munari (1991c) seems to support a variability of the carbon giant with a period of  $\sim 55$  days. If confirmed, this would be among the shortest period known for carbon pulsating variables (cf. Claussen et al. 1987). MHZ report  $B = 18.6$  and  $B - V = +1.5$  mag.

**ALS 2.** Its symbiotic nature has been discovered by Acker et al. (1988). MHZ lists  $B = 16.2$  and  $B - V = +1.9$  mag. The orbital period, type of variability and presence of historical outburst are unknown.

**FG Ser.** After the 1988–1994 outburst when it rose to  $B = 10.4$  and  $B - V = +1.1$ , it is now back toward the quiescent  $B = 13.8$  and  $B - V = +2.0$  mag values. MHZ list  $B = 13.5$  and  $B - V = +1.7$  mag. Munari et al. (1992b) discovered eclipses during the outburst phase (of amplitude  $\Delta V = 1.4$ ,  $\Delta B = 1.9$ ,  $\Delta U = 2.3$  mag and 120 days between first and fourth contact). From three consecutive minima Munari et al. (1995) derived the following ephemeris

$$T(\text{min}) = 2448492(\pm 4) + 658(\pm 4) \times E \quad (6)$$

where 658 is the period in days, as usual. From 250 archive blue plates covering the period 1949–1987, Kurockin (1993) found a large and sinusoidal variability at quiescence ( $\Delta B = 1.5$  mag), following the ephemeris

$$T(\text{min}) = 2446591 + 630 \times E \quad (7)$$

which could be interpreted in terms of a reflection effect. The difference between the two periods (both should trace the orbital period) has to be investigated. It should also be noted that the cool component does not show intrinsic or ellipsoidal variability in excess of 0.1 mag. The eclipses have not yet been searched for during quiescence. Their detection and monitoring would be of interest to measure the size, temperature and luminosity of the white dwarf now that it is returning back to quiescence dimensions.

**V443 Her.** No outburst has ever been recorded from this fairly bright symbiotic star. Its behavior in quiescence has been investigated by Kolotilov et al. (1995) who found a lightcurve dominated by a reflection effect of  $\Delta U = 0.9$ ,  $\Delta B = 0.4$  and  $\Delta V = 0.1$  mag amplitude. The minima follow the ephemeris

$$T(\text{min}) = 2443660(\pm 30) + 594(\pm 3) \times E. \quad (8)$$

There seems to be another periodicity of no easy interpretation at 430 days. The mean values in quiescence are  $B = 12.5$  and  $B - V = +1.0$ . Limited infrared observations by Kolotilov et al. (1998) seems to argue against variability of the cool giant or an ellipsoidal distortion of it.

**K 3-9.** Originally classified among the planetary nebulae, its symbiotic star nature has been discovered by Acker et al. (1983). According to Ivison & Seaquist (1995) K 3-9 is among the brightest symbiotic radio sources, and could harbor a Mira variable and a WD locked in a permanent outburst state. A thick dust cocoon should encircle the binary system, and a huge external ionized nebular material completely dominates the optical spectra. The photometric properties, history and orbital period are unknown. MHZ report  $B = 18.3$  and  $B - V = +1.3$ .

**MWC 960.** This is a bright symbiotic star neglected by the observers. Munari et al. (1992a) report  $B = 13.6$  and  $B - V = +1.5$  and MHZ list  $B = 13.8$  and  $B - V = +1.6$ . The photometric properties, history and orbital period are unknown.

**AS 323.** Another object originally classified as a planetary nebula which later turned out to be a symbiotic star (Sabbadin 1986; Acker et al. 1983). MHZ report  $B = 15.2$  and  $B - V = +1.0$ . The photometric properties, history and orbital period are unknown.

**FN Sgr.** Another bright symbiotic star that has been overlooked by most observers even though reports of large variability date back to Ross (1926). Outbursts have been recorded in 1924–1926 and 1936–1941. The brightness in quiescence seems to vary by a large amplitude ( $\Delta m \sim 2$  mag) with possible periodicities between 1 and 3 years (cf. Kenyon 1986 and references therein). Amateur visual observations over the last few years show a pattern reminiscent of an eclipsing binary following the ephemeris (Munari et al., in preparation):

$$T(\text{min}) = 2451410(\pm 15) + 1120(\pm 20) \times E. \quad (9)$$

The mean brightness is  $V \sim 13.5$  in eclipse and  $V \sim 11.0$  outside. Next minimum is scheduled for mid September 2002. MHZ list  $B = 12.7$  and  $B - V = +0.7$ .

**V919 Sgr.** Another bright object ignored by observers. According to literature review and new observations by Ivison et al. (1993), V919 Sgr varies between  $B = 12$  and  $B \geq 14.2$  mag. Its cool giant is definitively variable in the infrared by at least  $\Delta K = 0.7$  mag. The announcement of an outburst was made in 1991, but it is not yet proven it actually occurred (see Ivison et al. 1993). MHZ report  $B = 14.2$  and  $B - V = +1.2$ . The past photometric history and orbital period are unknown.

**CM Aql.** Another relatively bright symbiotic star that has been overlooked by most observers. Its range of variability extend from  $B = 13.0$  to  $B = 16.5$ . Outbursts have been reported for 1914, 1925, 1934, 1950. CM Aql also attracted some attention in late 1992 when from the usual  $V = 13.2$  it rose for a short period to  $V \sim 12$  mag. The orbital period is unknown. MHZ report  $B = 14.6$  and  $B - V = +1.3$ .

V1413 Aql. The star erupted into a symbiotic nova in late 1981, and has not yet returned to quiescence conditions. According to Munari (1992), V1413 Aql presented in quiescence one of the largest known reflection effects ( $B$  varying between 16.5 and 14.0 mag). When the star erupted into outburst, deep eclipses appeared perfectly in phase with the minima of the reflection effect according to the ephemeris

$$T(\text{min}) = 2446650(\pm 15) + 434.2(\pm 0.2) \times E. \quad (10)$$

At outburst maximum the star peaked at  $B = 11.2$  and  $B - V = +0.7$  (compared to  $B = 15.5$  and  $B - V = +1.5$  in quiescence). The decline has been very slow but smooth until late 1992 when V1413 Aql went back on the rise and returned to peak brightness ( $V = 10.5$ ) by summer of 1995 and started to decline again in a very smooth way (Munari 1996). The eclipses have always been visible during the whole outburst phases since 1982, and at minimum the star shines at  $V \sim 15.0$ . Outside eclipses the star is currently at  $V = 13.1$  and  $B - V = +0.9$ . If the present rate of decline of  $\Delta V = 0.56 \text{ mag yr}^{-1}$  will be maintained in the future, the star should return to quiescence brightness by late 2002. A detailed multi-band monitoring of successive eclipses would be of great interest to model the radius, temperature and luminosity of the outbursting component while it is returning back to quiescence conditions.

Ap 3-1. Another example of an object originally classified as a planetary nebula, and which later turned out to be a symbiotic star (Allen 1984). Its photometric properties are unknown. MHZ list  $B = 19.1$  and  $B - V = +2.1$ .

ALS 1. Its symbiotic nature has been discovered by Acker et al. (1988), who report  $V = 14.8$  mag. MHZ lists  $V = 13.5$  and  $B - V = +1.4$  mag. The photometric properties, history and orbital period are unknown.

V335 Vul. A symbiotic nature for this carbon star has been suggested only recently (Munari et al. 1999a). The star colors are very red, with MHZ giving  $V = 12.9$  mag and  $B - V = +5.1$  for quiescence. Munari et al. (1999b) caught the star on the rising branch of an apparent outburst, with  $V = 11.3$  and  $B - V = +3.1$  and a ten-fold increase in the intensity of emission lines. The orbital period is unknown. According to Dahlmark (1993) the carbon star is a Mira variable of  $10.5 < V < 13.2$  range, and maxima given by the ephemeris

$$T(\text{max}) = 2446740 + 342(\pm 0.2) \times E. \quad (11)$$

The possible outburst reported by Munari et al. (1999b) for the end of 1999 happened at the time of maximum brightness for the Mira variable (O. Pejcha and P. Sobotka, private communication). The puzzling coincidence of the two events should be studied in more details.

QW Sge. Examining 438 archive blue plates covering the period 1960-1992, Kurockin (1993) has discovered two outbursts: one extending from July 1962 to March 1972 with  $B = 11.5$  at maximum, the other from May 1982 to September 1989 with a much more complex lightcurve and

a peak brightness  $B = 12.0$ . Outside outburst phases the star is since first observations in 1898 at  $B \sim 13.1 \div 13.3$ . MHZ lists  $B = 13.2$  and  $B - V = +0.81$  mag. QW Sge has an optical companion 3.5 arcsec to the north, that Munari & Buson (1991) classified as an F0 V star with  $B = 13.59$  and  $B - V = +0.45$ . Our photometry gives different values,  $B = 13.18$  and  $B - V = +0.83$ , with a large scatter of 0.25 mag between three different measurements (compared to the few millimag for nearby stars of similar brightness). All this suggests that the optical companion is itself a variable star, and this complicates the interpretation of photometry made with moderate or short focus telescopes that are not able to separate QW Sge from the close optical companion (as it is the case for most of the archive photographic plates). It seems relevant to observe QW Sge with enough spatial resolution to avoid contamination from the nearby companion and to characterize the type and amplitude of variability of the latter. If the companion should turn out to be a moderate-amplitude variable and/or of a predictable type (like an eclipsing system), it would be possible to remove its contribution from the photographic photometry collected on QW Sge over the last century. No orbital period has been determined for QW Sge.

LT Del. A large reflection effect ( $\Delta U = 1.6$ ,  $\Delta B = 0.5$  and  $\Delta V = 0.2$  mag) following the ephemeris

$$T(\text{min}) = 2445910(\pm 5) + 478.5(\pm 2) \times E \quad (12)$$

has been discovered by Arkhipova et al. (1995), who lists  $B = 14.4$  and  $B - V = +1.3$  mag as mean values for the quiescence. MHZ report  $B = 14.3$  and  $B - V = +1.3$ . The only recorded outburst of LT Del has been discovered in the summer of 1994 by Passuello et al. (1994), when the star rose to  $B = 12.8$  and  $B - V = +0.5$ . The star has returned to quiescence by early 1998.

Hen 2-468. The photometric properties, history and orbital period are unknown. MHZ list  $B = 16.6$  and  $B - V = +1.8$  mag.

V407 Cyg. Discovered as Nova Cyg 1936, it was found by Meinunger (1966) to harbor a Mira variable with one of the longest pulsation period known and maxima following the ephemeris

$$T(\text{max}) = 2429710 + 745 \times E. \quad (13)$$

While reconstructing the historical lightcurve, Munari et al. (1990) discovered that brightness at the maximum of the pulsation cycle is strongly modulated by a sinusoidal variation with a possible period around 43 years and extrema at  $B_{\text{max}} = 13.3$  and  $B_{\text{max}} = 17.0$ . The 43 year periodicity was interpreted as the orbital period of the system. V407 Cyg was discovered again in outburst in the summer of 1994 by Munari et al. (1994), when it rose to  $B = 14.0$  and  $B - V = +1.0$  (same value as in the 1936 outburst) at a time when contemporaneous infrared photometry confirmed that the Mira was at a minimum in its pulsation cycle. According to VSNET databank the last minimum of the Mira has been in the very early 1998

( $V > 16.0$ ) and the last maximum in June 1999 ( $V \sim 11.2$ ). The lightcurve is however quite complicated with humps as large as one magnitude superimposed to the much smoother lightcurve of the Mira. The humps are possibly connected with the current enhanced activity phase of the white dwarf and would deserve close monitoring over the whole  $UBV(RI)_C$  range. MHZ list  $B = 13.2$  and  $B - V = +1.5$ .

V627 Cas. Originally classified among the T Tau pre-main sequence variables, its symbiotic star nature was discovered by Kolotilov (1988). Kolotilov et al. (1996) has summarized the optical and infrared photometric properties of V627 Cas. The cool component seems to be a M2 supergiant in a post-AGB phase, pulsating with a 466 day period. The hot component presents flickering activity superimposed onto several different types of variability, including a secular dimming by  $\Delta B = 2.0$  mag in 60 years. This is a peculiar type of symbiotic star which needs more effort to be better characterized from a photometric point of view. To null the effect of flickering, the star should be observed more times per night and over a few consecutive nights in all the  $UBV(RI)_C$  bands.

StH $\alpha$  32. Its symbiotic star nature has been discovered by Downes & Keyes (1988). The photometric properties are unknown. MHZ list  $B = 14.2$  and  $B - V = +1.4$ .

## References

- Allen D.A., 1984, Proc.A.S.A. 5, 369  
 Aaronson M., Liebert J., Stocke J., 1982, ApJ 254, 507  
 Acker A., Lundström I., Stenholm B., 1988, A&AS 73, 325  
 Arkhipova V.P., Ikonnikova N.P., Noskova R.I., 1995, PAZh 21, 379  
 Clausaen M.J., Kleinmann S.G., Joyce R.R., Jura M., 1987, ApJS 65, 385  
 Dahlmark L., 1993, IBVS 3855  
 Downes R.A., Keyes C.D., 1988, AJ 96, 777  
 Henden A.A., Kaitchuck R.H., 1990, Astronomical Photometry. Richmond: Willmann-Bell  
 Ivison R.J., Seaquist E.R., 1995, MNRAS 272, 878  
 Ivison R.J., Munari U., Marang F., 1993, A&A 277, 510  
 Kenyon, 1986, The Symbiotic Stars. Cambridge University Press  
 Kolotilov E.A., 1988, Astrofizika 9, 458  
 Kolotilov E.A., Munari U., Yudin B.F., 1995, A&A 293, 815  
 Kolotilov E.A., Munari U., Yudin B.F., Tatarnikov A.M., 1996, Sov. Astron. 40, 812  
 Kolotilov E.A., Munari U., Popova A.A., Yudin B.F., 1998, Astron. Lett. 24, 34  
 Kurochkin N.E., 1993, Astron. Astrophys. Trans. 3, 295  
 Landolt A.U., 1983, AJ 88, 439  
 Landolt A.U., 1992, AJ 104, 340  
 Meinunger L., 1966, Mitt. Veranderl. Sterne 3, 111  
 Munari U., 1991a, Inf. Bull. Var. Stars 3605  
 Munari U., 1991b, A&A 251, 103  
 Munari U., 1991c, Inf. Bull. Var. Stars 3648  
 Munari U., 1992, A&A 257, 163  
 Munari U., 1996, in Physical Processes in Symbiotic Binaries and Related Systems, Mikolajewska J. (ed.). Polish Academy of Sciences, p. 37  
 Munari U., Margoni R., Stagni R., 1990, MNRAS 242, 653  
 Munari U., Buson L.M., 1991, A&A 249, 141  
 Munari U., Yudin B.F., Taranova O.G., et al., 1992a, A&AS 93, 383  
 Munari U., Whitelock P.A., Gilmore A.C., et al., 1992b, AJ 104, 262  
 Munari U., Bragaglia A., Guarnieri M.D., Sostero G., Lepardo A., Yudin B.F., 1994, IAU Circ. 6049  
 Munari U., Yudin B.F., Kolotilov E.A., Gilmore A.C., 1995, AJ 109, 1740  
 Munari U., Rejkuba M., Mattei J., Hazen M., Luthardt R., Yudin B.F., 1997, A&A 323, 113  
 Munari U., Tomov T., Rejkuba M., 1999a, IBVS 4668  
 Munari U., Tomov T., Moro D., Henden A., 1999b, IAU Circ. 6065  
 Passuello R., Saccavino S., Munari U., 1994, IAU Circ. 6065  
 Ross F.E., 1926, AJ 36, 122  
 Sabbadin F., 1986, A&AS 65, 301  
 Stetson P.B., 1987, PASP 99, 191  
 Wallace P., 1994, in Astronomical Data Analysis Software and Systems III, PASP Conf. Ser. 61, Crabtree D.R., Hanisch R.J. and Barnes J. (eds.). San Francisco: ASP, p. 481